

Production of nanoparticles of copper compounds by anodic dissolution of copper in organic solvents

B. STYPUŁA¹, J. BANAS¹, M. STAROWICZ^{1,*}, H. KRAWIEC¹, A. BERNASIK² and A. JANAS³

¹Department of General and Analytical Chemistry, AGH – University of Science and Technology, Reymonta 23, 30-059, Krakow, Poland

²Faculty of Physics and Applied Computer Science, AGH – University of Science and Technology, Reymonta 19, 30-059, Krakow, Poland

³Faculty of Foundry Engineering, AGH – University of Science and Technology, Reymonta 23, 30-059, Krakow, Poland

(*author for correspondence, tel.: +4812-6174120, fax: +4812-6336348, e-mail: mariast@agh.edu.pl)

Received 10 June 2005; accepted in revised form 22 August 2006

Key words: anodic dissolution in ethanol, copper compounds, copper dissolution, copper oxide nanoparticles, organic solvents

Abstract

The anodic behaviour of copper was investigated in ethanol solution containing LiClO₄, LiCl electrolyte and water. The type of electrolyte and the water content influences the mechanism of the anodic process and the formation of anodic products. In LiClO₄ electrolyte the dissolution of copper is related to the oxidation of Cu(I) to Cu(II). In solutions of LiCl the etching of copper begins with the creation of soluble complexes of Cu(I) with chloride ions and solvent molecules. At potentials above 0.4 V the formation of alkoxides was observed in both solutions, characterized by a yellow tint. On the other hand, above 0.8 V (i.e. above the equilibrium potential of alcohol oxidation) copper dissolution is accompanied by the formation of a blue colloidal suspension of Cu (II) copper salt. Anodic etching of copper in solutions containing 3% H₂O at potentials higher than 0.4 V leads to the formation of colloidal suspension of copper oxide nanoparticles.

1. Introduction

The electrochemical behaviour of copper in organic solvents has been studied extensively during the last few years owing to the scientific and technological importance of the metal and its compounds, especially in the field of catalysis, battery technology and electronics [1, 2].

Recently, nanoparticles of copper compounds, particularly oxides, have received increased attention, because of their special properties such as a large surface to volume ratio, increased activity, electronic properties and unique optical properties as compared to those of bulk materials. The oxides of copper (Cu₂O and CuO) constitute an important class of semiconductors, which are applied in magnetic storage media, solar energy conversion, electronics and catalysis [3–5]. Some methods for the preparation of nanoparticles such as thermal and sonochemical reduction [6, 7], microwave irradiation [8], thermal decomposition of precursors [9], the sol–gel technique [10], the one step solid state reaction at room temperature [11] and the electrochemical method [12] have been reported.

The purpose of the present work was to study the anodic behaviour of copper in organic solvents and search for a possible synthesis of nanoparticles via an electrochemical method. We have studied the anodic behaviour of Cu over a wide range of potential values in organic solvents.

2. Experimental

Samples of metallic copper (99.99% Cu), were polished using abrasive paper in decreasing order of grain size. Before electrochemical treatment copper electrodes were cleaned in anhydrous ethanol. Chemical reagents: LiClO₄ (99.8%) and LiCl (99.8%) both from Merck and anhydrous ethanol (99.8%) from EUROCHEM BGD, were used in the preparation of solutions.

The studies were performed in 0.1 M LiClO₄ as well as in 0.1 M, 0.01 M and in 0.05 M LiCl solutions. In order to study the effect of water some of these solutions contained 1% or 3% of H₂O.

The anodic properties of copper were investigated at room temperature using a PGZ301 Voltalab potentiostat by means of the potentiostatic (chronoamperometry)

and potentiodynamic technique (cyclic voltammetry). The experiment was performed in three electrode systems with the solution deaerated by pure argon. A circular flat surface of copper (5 mm diameter) was used as working electrode, a platinum foil served as counter electrode and Ag/AgCl used as reference electrode. The potentials in this paper are versus Ag/AgCl unless another reference is given. Potentiodynamic polarization sweeps of the working electrode were performed at a rate of 1, 3 and 5 V min⁻¹. Potentiostatic studies were carried out at 0.2 V to 1 V for 2 to 4 h.

Precipitated products of anodic dissolution were analysed by means of scanning electron microscopy with energy dispersive X-ray analysis (SEM/EDX), transmission electron microscopy TEM and X-ray photoelectron spectroscopy (XPS). SEM and EDX analysis were performed by a JEOL 5500 LV instrument. TEM images were recorded using a Phillips CM20 TWIN (200 kV) instrument.

XPS measurements were performed using an ESCA – VSW spectrometer. Mg K_α – radiation of 1253.6 eV at a power of 200 W was used. The base pressure used during the analysis was below 3 × 10⁻⁸ mbar. The high-resolution spectra were recorded with electron pass energy of 22 eV. All spectra were calibrated by using the adventitious carbon C1s peak at binding energy (*E_B*) equal to 284 eV. The diameter of the analysed area was 3 mm.

The relative element content was calculated using the formula (1) according to [13]

$$C_k = \frac{I_k/\sigma_k}{\sum_i I_i/\sigma_i} \quad (1)$$

where, *C_k* – relative atomic concentration of element, *k* *I_k* – intensity of line *k*, *σ_k* – elemental cross-section for photoionisation.

Precipitated copper compounds were separated from the solution by decantation. Subsequently, wet solids were placed on a Pt or Zn plate, dried at room temperature and characterized by SEM/EDX analysis. Samples for TEM and XPS analysis were prepared by putting a drop of the colloidal solutions on a carbon grid or plate, respectively. The wet sample was transferred to the vacuum chamber quickly with care to avoid oxidation.

3. Results and discussion

3.1. Anodic process in LiClO₄-C₂H₅OH electrolyte

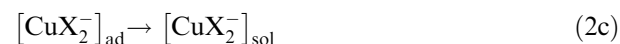
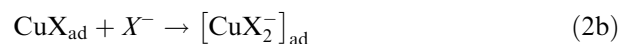
The anodic behaviour of copper in non-aqueous ethanol containing LiClO₄ is shown in Figure 1. Copper undergoes anodic etching without the formation of a passive oxide layer in non-aqueous solutions of 0.1 M LiClO₄, in ethanol as well as methanol [14]. There is general agreement in the literature [14–17] that copper dissolution in both aqueous and non-aqueous media proceeds in two steps:



The anodic polarisation curves in LiClO₄-C₂H₅OH electrolyte can be divided into five distinct regions (Figure 1):

- (I) The oxidation region (between -0.7 V and approximately -0.5 V)
- (II) The limiting current region (between -0.5 V and 0.2 V)
- (III) The second oxidation and active dissolution region (with a maximum at about 0.3 V)
- (IV) The second limiting current region (between 0.3 V and 0.8 V)
- (V) The aggressive dissolution region (above 0.8 V)

The shape of the curves in the initial part of the anodic range (Figure 1) appears similar to that in the aqueous solution containing chloride ions, presented by Itagaki and co-workers [17]. In accordance with the reference [17] and our earlier work [18] copper dissolution in the first region (Figure 1) can be presented as the formation of monovalent Cu(I) coordinated by anions and/or ethoxy groups (X⁻). The following dissolution mechanism is proposed:



The monovalent Cu complexes adsorbed on the surface play an important role as an intermediate in both the dissolution and deposition processes [19, 20]. In the anhydrous ethanol Cu(I) is stable in the limiting current region (Figure 1, region II). The presence of Cu(I) is supported by a lack of colour of the solution,

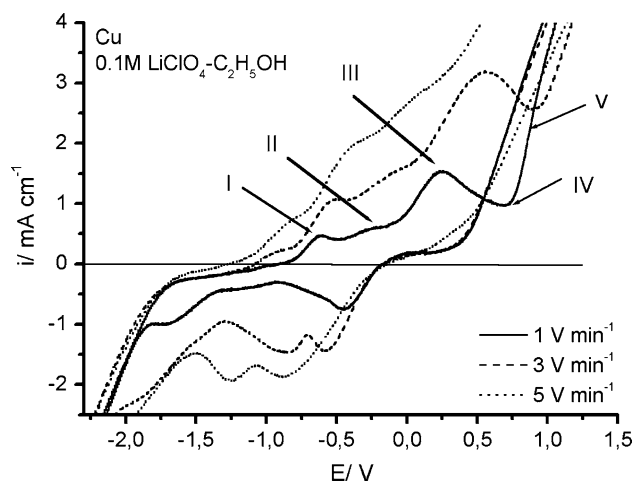


Fig. 1. Polarization curves of copper in anhydrous 0.1 M LiClO₄-C₂H₅OH.

Table 1. The colour of the solution after polarisation of copper in 0.1 M LiClO₄-C₂H₅OH

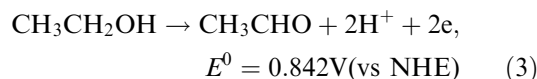
Potential and time of polarisation	Colour of solution
200 mV, <i>t</i> = 120 min	Transparent
400 mV, <i>t</i> = 120 min	Yellow-green
1000 mV, <i>t</i> = 120 min	Blue

following anodic copper polarization at potentials in region I or II (Table 1).

The dissolution process in the limiting current region II is almost the same as in region I. The difference is in the fractional coverage of the surface by Cu(I) compounds. The linear relationship between the anodic peak current densities and scan rate (Figure 2) indicates adsorption control of the anodic process. In the case where the adsorption can be described by the Langmuir isotherm the peak current density is a linear function of the polarisation rate [21].

The second oxidation region has a wide maximum around 0.3 V (Figure 1). The anodic dissolution of copper in this region, proceeds intensively and coincides with stronger etching of a copper surface and the formation of Cu(II) compounds [18]. The soluble copper product gives the characteristic yellow-green colour of the solution (Table 1). The decrease in anodic current density in region IV (Figure 1) may be related to the formation of a Cu(II) compound layer on the copper surface. In aqueous solutions the potential of copper (I) oxidation is $E_{\text{Cu}^+/\text{Cu}^{2+}}^0 = 0.16 \text{ V}$ (vs. NHE) and the potential of Cu(II) formation is $E_{\text{Cu}/\text{Cu}^{2+}}^0 = 0.34 \text{ V}$ (vs. NHE).

At higher potential values, above approximately 0.8 V (region V, Figure 1) the dissolution rate increases sharply with increase in potential. This increase can be related to the oxidation of the alcohol solvent to the aldehyde in accordance with the general equation:



Oxidation of alcohol results in a modification of the environment and causes a change in the anodic process and the formation of anodic copper oxidation products. This is confirmed by the change of solution colour during chronoamperometric polarization. The anolyte changes colour from yellow through yellow-green to blue. The last colour is characteristic of solvated Cu(II) ions (Table 1). The mechanism of anodic dissolution of copper in the range of high potentials is not known so far and requires further research.

3.2. Anodic process in LiCl-C₂H₅OH solutions

The curve for the anodic polarization of copper in ethanol solution containing chloride ions is different from that in LiClO₄ solution, especially at low potentials (Figure 3). Chloride ions inhibit anodic copper dissolution in the first region. This behaviour indicates higher stability of the surface Cu(I) compounds in this potential range in the presence of chloride ions.

In the higher potential range, above -0.2 V, the current density increases with increase in chloride ion concentration. The reaction order versus chloride concentration (at 0.2 V) is approximately one and increases with potential (Figure 4). This suggests that the sparingly soluble CuCl, formed in the initial stages, is introduced to the solution as readily soluble $[\text{CuCl}_2]_{\text{sol}}^-$ complexes with chloride ions and/or $[\text{CuCl}_2\text{OEt}]_{\text{sol}}^{2-}$ containing ethoxy groups from the solvent. This is due to intensive copper etching in chloride solutions at potentials above -0.2 V. The formation of soluble complexes of monovalent copper is confirmed by the lack of electrolyte colour up to 0.4 V (Table 2). At higher potentials, $E \geq 0.4 \text{ V}$, the anolyte changes colour from yellow to blue, as in LiClO₄ solution (Table 1 and

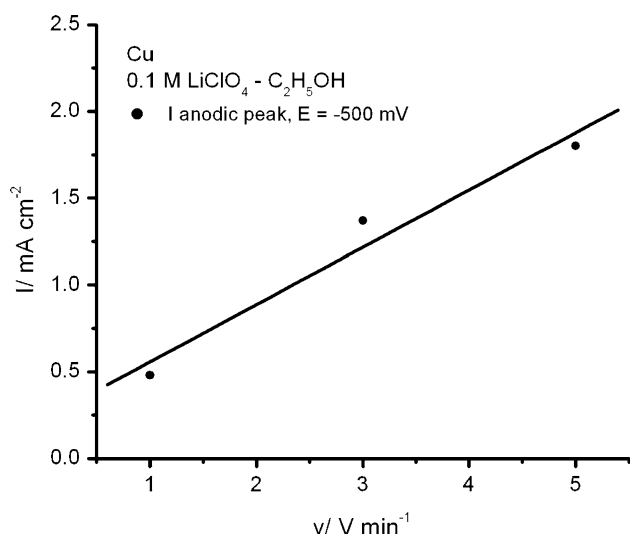


Fig. 2. Dependence of anodic peak current density on polarization rate.

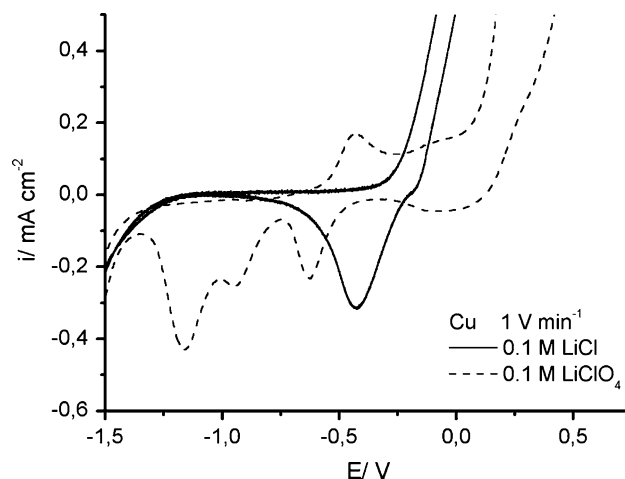


Fig. 3. Polarization curves of Cu in anhydrous 0.1 M LiCl-C₂H₅OH and 0.1 M LiClO₄-C₂H₅OH.

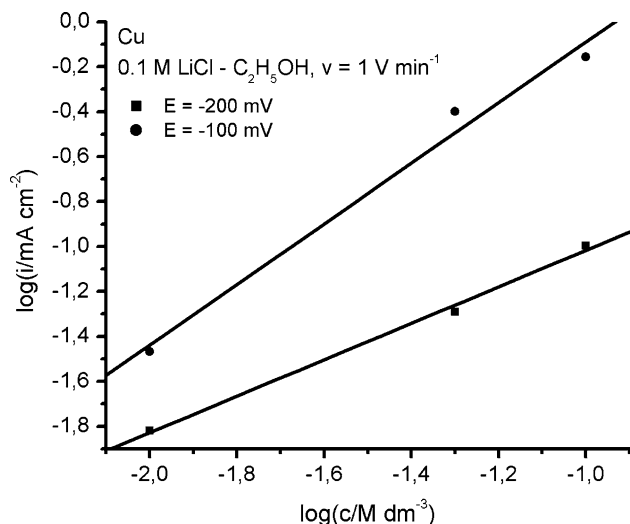


Fig. 4. Dependence of anodic active dissolution current density on the concentration of chloride ions.

Table 2). It is worth noting that during long polarisation, at $E \geq 0.6$ V, the dissolution of copper in LiCl solutions leads to the formation of a colloidal solution and a precipitate (Table 2).

TEM and SEM/EDX analysis of the precipitate is presented in Figure 5 and Table 3. The blue colour of the precipitate and high molar ratio of oxygen to copper content suggests the formation of nanoparticulate copper acetate or other organic compounds.

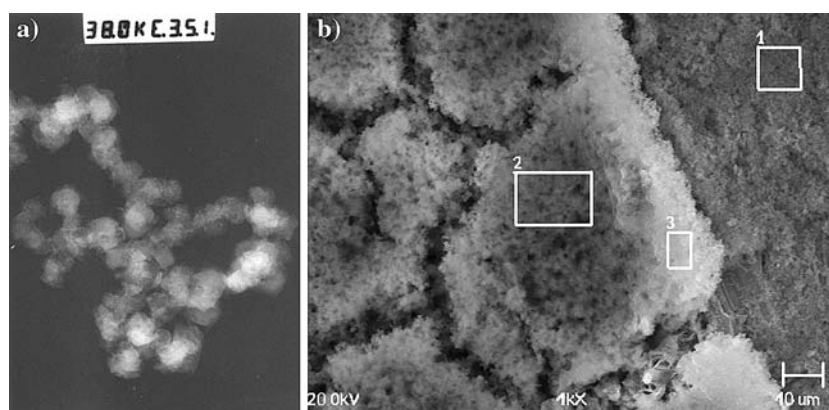


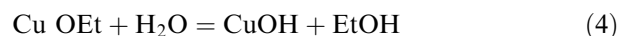
Fig. 5. TEM analysis (a) and SEM/EDX analysis (b) of the precipitate formed in 0.1 M LiCl–C₂H₅OH at 1 V (blue powder).

Table 2. Colouring of the electrolyte during chronoamperometric polarization of copper

Solution	Colour of solution or precipitate		
	Potential/mV	Time 2 h	Time 4 h
0.1 M LiCl–C ₂ H ₅ OH	200	Colourless	Colourless, transparent
0.1 M LiCl–C ₂ H ₅ OH	400	Light yellow	Yellow solution
0.1 M LiCl–C ₂ H ₅ OH	600	Yellow–green	Dark blue colloidal
0.1 M LiCl–C ₂ H ₅ OH	800	Blue colloidal	Blue powder
0.1 M LiCl–C ₂ H ₅ OH	1000	Blue colloidal	Blue powder
0.1 M LiCl–C ₂ H ₅ OH + 3% H ₂ O	400		Yellow–orange powder
0.1 M LiCl–C ₂ H ₅ OH + 3% H ₂ O	600		Yellow–orange powder
0.1 M LiCl–C ₂ H ₅ OH + 3% H ₂ O	800		Yellow–brown powder
0.1 M LiCl–C ₂ H ₅ OH + 3% H ₂ O	1000		Brown powder

3.3. The influence of water content on anodic process

Water addition up to 3 wt % does not have significant effect on the mechanism of copper dissolution in chloride which shows that the coordination process using chloride ions dominates in this environment (Figure 6). The inhibiting effect of water on the anodic process was observed in perchlorate solutions (Figure 7). The presence of water may additionally influence the change of the coordination sphere of the anodic products at high potentials. At potentials above 0.4 V yellowish anolyte becomes an opaque colloidal form. The colour of the colloidal copper compounds changes from yellow (yellow orange) to brown during chronoamperometric polarization at potentials higher than 0.4 V (Table 2). Similar colouring of solution accompanied the synthesis of copper oxide Cu₂O nanoparticles in a chemical process [22, 23]. These results show that the anodic product – Cu(I) alkoxide or/and Cu(I) alkoxide complexes undergo hydrolysis in the presence of water:



The formation of copper(I) oxide nanoparticles may proceed according to the subsequent reactions:

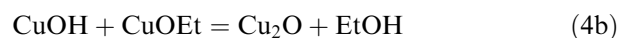
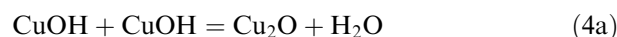


Table 3 EDX analysis of the blue powder (after Cu polarisation in 0.1 M LiCl-C₂H₅OH at 1000 mV, t = 4 h for Figure 5)

	Cu	O	Cl
Atomic %			
Area 1	16.3 (±1.7)	83.1 (±1.7)	0.6 (±0.1)
Area 2	25.4 (±2.5)	71.4 (±1.9)	3.2 (±0.4)
Area 3	12.8 (±2.0)	86.1 (±2.2)	1.1 (±0.2)

SEM/EDX analysis of the precipitate (Figure 8, Figure 9, Table 4 and Table 5) confirms that copper oxide nanoparticles are formed at potentials higher than 0.4 V. The ratio O/Cu is higher than 1/2 (Table 4 and 5), but it is most probably influenced by the adsorption of ethanol on the nanoparticle surface. Additionally, SEM/EDX analysis shows the presence of a significant amount of chlorine. The chlorine content diminishes significantly to approximately 3% after rinsing the precipitate with alcohol (Figure 10 and Table 6), which suggests that chlorine only accumulated at the particle surfaces.

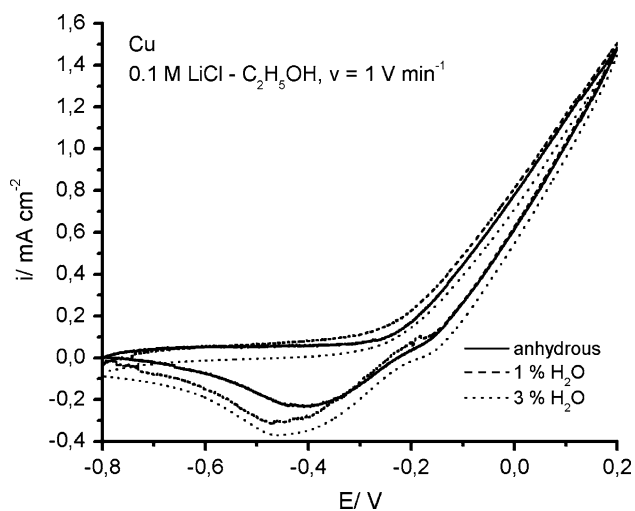


Fig. 6. Influence of water on the polarization of Cu in ethanolic solution of LiCl.

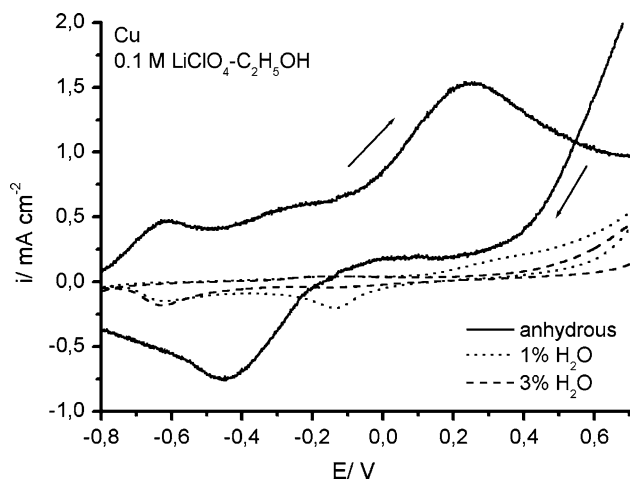


Fig. 7. Influence of water on the polarization of Cu in ethanolic solution of LiClO₄.

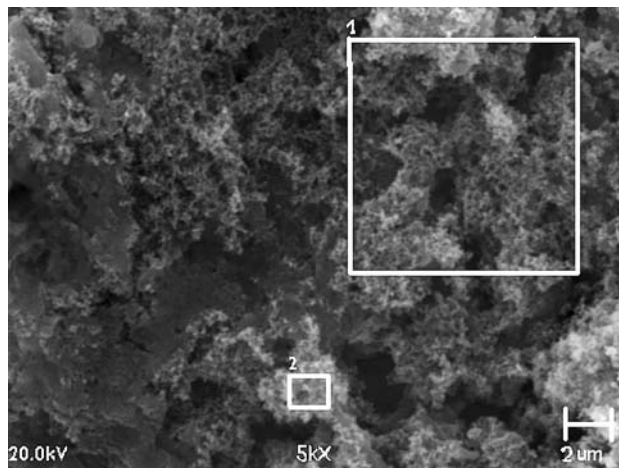


Fig. 8. SEM/EDX analysis of the precipitate formed in 0.1 M LiClO₄-C₂H₅OH + 3% H₂O at 1 V (brown powder).

3.4. XPS-investigation of nanoparticles

3.4.1. 0.1 M LiCl-C₂H₅OH (1.0 V) – blue powder

Figure 11(a) shows the Cu 2p spectra for the blue nanoparticles obtained in the 0.1 M LiCl-C₂H₅OH anhydrous solution at a potential of 1.0 V. Table 7 collects corresponding values of electron binding energy. The good fit of the Cu 2p^{3/2} spectrum can be obtained with two peaks. The one at the lower energy (933.0 eV) agrees with the peak position for Cu (II) in copper oxide. The second one at 934.5 eV corresponds to Cu (II) in copper oxo-salts [24–26]. In addition, the spectra show the presence of satellite peaks at higher binding energy with respect to the main peaks (Table 7). The existence of a strong satellite in the Cu2p band clearly shows that the nanoparticles consist of Cu (II) compounds. The O 1s spectra can be arbitrarily decomposed into three peaks at about ~530, ~532 and ~533 eV, (Figure12). These values may correspond first to the oxygen in oxides, second to the oxygen in oxyanions or the carboxylate group and third to oxygen in adsorbed ethanol or esters [27–29]. XPS spectra also show the

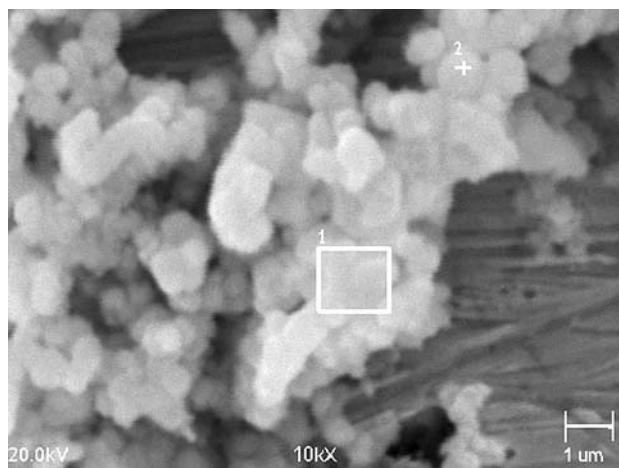


Fig. 9. SEM/EDX analysis of the precipitate formed in 0.1 M LiCl-C₂H₅OH + 3% H₂O at 1 V (brown powder).

Table 4. EDX analysis of the brown powder (after Cu polarisation in 0.1 M LiClO₄-C₂H₅OH + 3% H₂O at $E = 1000$ mV, $t = 4$ h for Figure 8)

	Atomic %		
	Cu	O	Cl
Area 1	36.2 (± 2.3)	52.8 (± 1.3)	10.9 (± 0.5)
Area 2	40.6 (± 2.7)	50.2 (± 1.4)	9.4 (± 0.5)

Table 5 EDX analysis of the brown powder (after Cu polarisation in 0.1 M LiCl-C₂H₅OH + 3% H₂O at $E = 1000$ mV, $t = 4$ h for Figure 9)

	Atomic %		
	Cu	O	Cl
Area 1	40.9 (± 3.0)	44.2 (± 1.4)	14.9 (± 0.7)
Area 2	39.1 (± 3.0)	46.8 (± 1.4)	14.1 (± 0.7)

Table 6. EDX analysis of the brown powder (after Cu polarisation in 0.1 M LiCl-C₂H₅OH + 3% H₂O at $E = 1000$ mV, $t = 4$ h) after rinsing in ethanol (for Figure 10)

	Atomic %		
	Cu	O	Cl
Area 1	44.1 (± 3.0)	52.8 (± 1.3)	3.1 (± 0.3)
Area 2	48.4 (± 3.1)	48.8 (± 1.3)	2.8 (± 0.3)

presence of Cl in chlorides and/or ClO_x groups ($E_B = 199.1$ eV, $E_B = 200.2$ eV) [30, 31].

XPS analysis (as well as SEM/EDX) shows that copper(II) salt and oxide with a possible amount of chloride are formed in anhydrous LiCl-C₂H₅OH, via copper etching at 1.0 V.

The differences in molar ratio Cu:O:Cl obtained by SEM and XPS techniques (see Table 3 and 7) are related to the fact that these methods probe different depths of a specimen and the information is collected over different areas. The XPS analysis concerns nano-range depth and the information is recorded over a large area, whereas SEM/EDX delivers data from a small area, with larger depth (micrometers) of analysis.

Table 7. XPS analysis of the blue powder obtained in 0.1 M LiCl-C₂H₅OH ($E = 1.0$ V, $t = 4$ h)

Level	E_B /eV experimental value	Atomic %	Compounds
Cu 2p	933.0 (± 0.5)	4.0	Cu(II) in oxide
	934.5 (± 0.5)	5.4	Cu(II) in salts
	941.5 (± 0.5)		Satellite
	944.0 (± 0.5)		Satellite
O 1s	530.6 (± 0.3)	21.4	O in oxides
	532.3 (± 0.3)	30.8	-C = O, O- in oxyanions
Cl 2p	533.8 (± 0.5)	10.5	-C-O- in C ₂ H ₅ OH
	199.1 (± 0.5)	25.2	Cl ⁻ in chlorides
	200.2 (± 0.5)	2.7	ClO _x

Table 8. XPS analysis of the yellow-brown powder obtained in 0.1 M LiCl-C₂H₅OH + 3% H₂O ($E = 0.8$ V, $t = 4$ h)

Level	E_B /eV experimental value	Atomic %	Compounds
Cu 2p	931.9 (± 0.2)	9.0	Cu (I)
	932.5 (± 0.5)	5.3	Cu (I) (Cu ₂ O)
O 1s	530.1 (± 0.5)	10.9	Oxides
	531.6 (± 0.5)	20.6	Cl-O-
	533.1 (± 0.5)	9.8	-C-O- in C ₂ H ₅ OH
Cl 2p	198.2 (± 0.5)	37.0	Cl ⁻ in CuCl
	199.3 (± 0.5)	7.5	Cl ⁻ in chlorides

Table 9. XPS analysis of the brown powder obtain in 0.1 M LiCl-C₂H₅OH + 3% H₂O ($E = 1.0$ V, $t = 4$ h)

Level	E_B /eV experimental value	Atomic %	Compounds
Cu 2p	932.4 (± 0.2)	9.3	Cu ₂ O
	934.1 (± 0.5)	5.8	Cu(II)
	942.4 (± 0.5)		Satellite
	943.0 (± 0.5)		Satellite
O 1s	530.2 (± 0.3)	28.9	Oxides
	531.8 (± 0.3)	21.6	Cl-O-
	533.4 (± 0.5)	5.6	-C-O- in C ₂ H ₅ OH
Cl 2p	198.5 (± 0.5)	22.0	Cl ⁻ in CuCl
	199.6 (± 0.5)	3.5	Cl ⁻ in chlorides

3.4.2. 0.1 M LiCl-C₂H₅OH + 3% H₂O (0.8 V) – yellow-brown powder

Figure 11b presents Cu2p spectra for the yellow-brown nanoparticles obtained in 0.1 M LiCl-C₂H₅OH containing 3% H₂O solution at 0.8 V. The Cu2p^{3/2} level consists of two peaks centered at 932.5 and 931.9 eV. According to the literature, these values indicate the presence of copper (I) compounds, Cu₂O and CuCl, respectively [32].

The presence of these compounds in the powder can be confirmed by the analysis of the Cl 2p and O 1s spectrum, (see Table 8). The higher E_B values of the

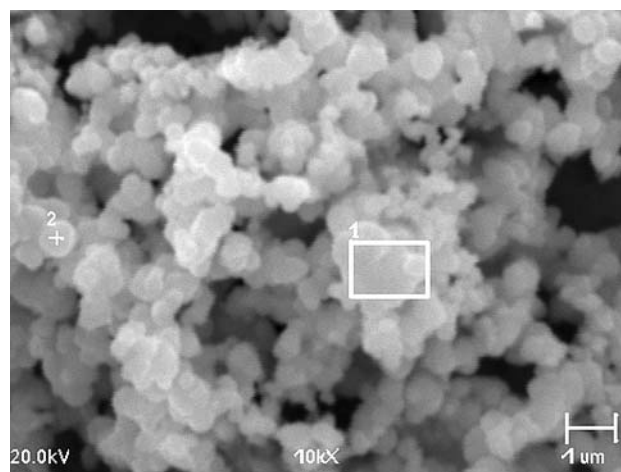


Fig. 10. SEM/EDX analysis of the precipitate formed in 0.1 M LiCl-C₂H₅OH + 3% H₂O at 1 V (brown powder) after rinsing in ethanol.

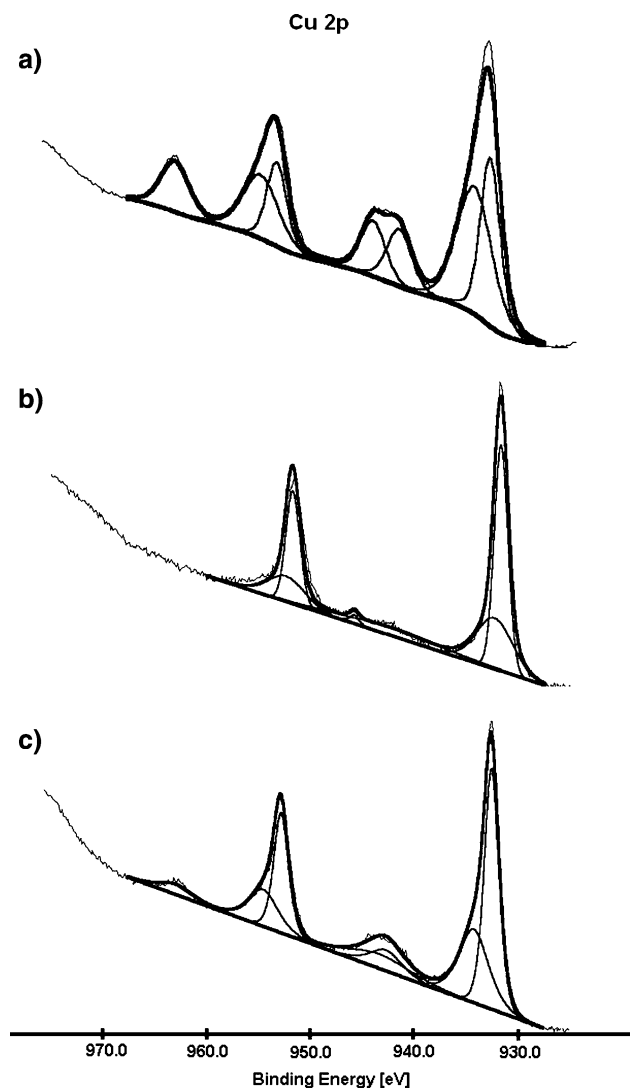


Fig. 11. XPS spectra of the Cu 2p region for: (a) blue powder obtained in 0.1 M LiCl-C₂H₅OH at 1.0 V; (b) yellow-brown powder obtained in 0.1 M LiCl-C₂H₅OH+3% H₂O at 0.8 V; (c) brown powder obtained in 0.1 M LiCl-C₂H₅OH+3% H₂O at 1.0 V.

peaks in the O1s band 531.6 and 533.1 eV are close to the binding energies of oxygen in the perchlorate and in the C₂H₅OH related bond, respectively [27].

The XPS results indicate the formation of Cu₂O nanoparticles with some CuCl during the anodic dissolution of copper in 0.1 M LiCl-C₂H₅OH solution containing 3% of water.

3.4.3. 0.1 M LiCl-C₂H₅OH+ 3% H₂O (1.0 V) – brown powder

The copper spectra of Cu2p for brown powder obtained in 0.1 M LiCl-C₂H₅OH solution containing 3% H₂O at 1.0 V are shown in Figure 11c and Table 9. In the spectrum of Cu2p^{3/2} an additional peak at 934 eV was observed apart from the peak at 932.4 eV originating from the Cu binding in Cu₂O (Table 9) [32]. The higher binding energy peak at

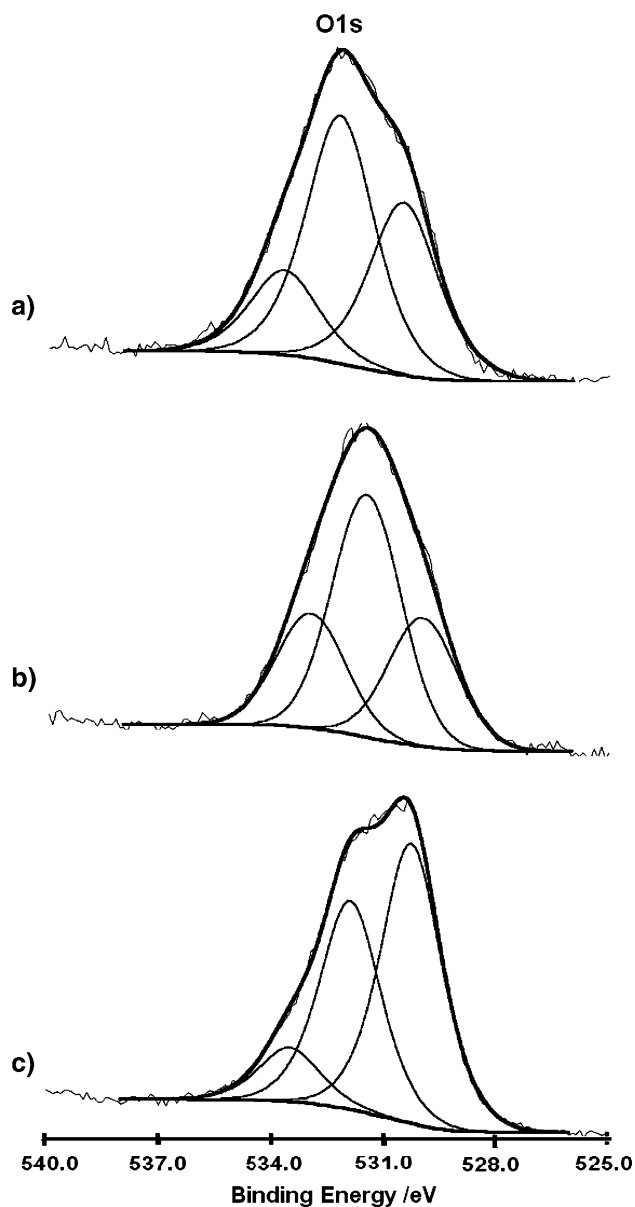


Fig. 12. XPS spectra of O 1s region for: (a) blue powder obtained in 0.1 M LiCl-C₂H₅OH at 1.0 V; (b) yellow-brown powder obtained in 0.1 M LiCl-C₂H₅OH+3% H₂O at 0.8 V; (c) brown powder obtained in 0.1 M LiCl-C₂H₅OH+3% H₂O at 1.0 V.

934 eV and the existence of a clear satellite indicate the presence of copper Cu (II) compounds [24–26]. The detected copper Cu(II) may result from the oxidation of Cu₂O on the surface. The spectra of Cl 2p and O 1s are nearly the same as in the case of yellow-brown powder.

Similarly as above, both methods (XPS and SEM/EDX) proved the formation of copper oxides during the anodic etching of copper in LiCl-C₂H₅OH solution containing 3% water. The high concentration of chlorine in the powder can be attributed to the chemisorption of chloride ions on the oxide nanoparticle surfaces.

4. Conclusion

- Copper rapidly undergoes aggressive anodic dissolution in ethanolic solutions of LiClO₄ and LiCl in the high potential region (>0.8 V).
- The composition of the anodic product and the valence of copper depend on potential and on the concentration of water in the electrolyte.
- In the anhydrous solution at 0.8 V nanoparticles of copper salts are an anodic dissolution product.
- In solution containing 3% H₂O at 0.8 V nanoparticles of Cu₂O are produced.
- In the same solution at 1 V nanoparticles of Cu₂O and a small amount of CuO are obtained.
- Anodic copper dissolution in ethanolic electrolytes is a novel and simple electrochemical production method of copper oxide nanoparticles.

Acknowledgements

This work was financed by the Polish Committee for Scientific Research (KBN) under project numbers 4 T08E 037 23 and 3 T08C 011 30.

References

1. W. Schafer and A.G. Dubinin, *Elektrokhimiya* **32** (1996) 333.
2. C. Javewardena, K.P. Hewaparakrama, D.L.A. Wijewardena and H. Guruge, *Sol. Energy Mater. Sol. Cells* **56** (1998) 29.
3. T. Maruyama, *Sol. Energy Mater. Sol. Cells* **56** (1998) 85.
4. W.P. Dow and T.J. Huany, *J. Catal.* **160** (1996) 171.
5. M. Frietsch, F. Zudock, J. Goek and M. Bruns, *Sensor Actuat. B-Chem.* **65** (2000) 379.
6. R.V. Kumar, Y. Diamant and A. Gedanken, *Chem. Mater.* **12** (2000) 2301.
7. N.A. Dhas, C.P. Raj and A. Gedanken, *Chem. Mater.* **10** (1998) 1446.
8. H. Wang, J.Z. Xu, J.J. Zhu and H-Y. Chen, *J. Cryst. Growth* **244** (2002) 88.
9. Z. Hong, Y. Cao and J. Deng, *Mater. Lett.* **52** (2002) 34.
10. A.A. Eliseev, A.V. Lukashin, A.A. Vertegel, L.I. Heifets, A.I. Zhironov and Y.D. Tretyakov, *Mater. Res. Innov.* **3** (2000) 308.
11. J.F. Xu, W. Ji, Z.X. Shen, S.H. Tang, X.R. Ye, D.Z. Jia and X.Q. Xin, *J. Solid State Chem.* **147** (1999) 516.
12. R.M. Penner, *J. Phys. Chem B* **106** (2002) 3339.
13. J.H. Scofield, *J. Electron Spectrosc. Related Phenomena* **8** (1976) 129.
14. K. Banaś, J. Banaś EUROCORR 96, session VIII, 8-I.
15. G. Lang, I. Bakos and G. Horanyi, *J. Electroanal. Chem.* **493** (2000) 141.
16. S. Magaino, *Electrochim. Acta* **42** (1997) 377.
17. M. Itagaki, M. Tagaki and K. Watanabe, *Corr. Sci.* **38** (1996) 1109.
18. B. Stypuła, J. Banaś, H. Krawiec, M. Starowicz, T. Habdank-Wojewódzki and A. Janas; *Ochrona przed korozją 11s/A/* (2004) 25.
19. J. Klunker and W. Schafer, *J. Electroanal. Chem.* **466** (1999) 107.
20. A. Vaskevich and I. Rubinstein, *J. Electroanal. Chem.* **491** (2000) 87.
21. R. Greef, R. Peat, L.M. Peter, D. Pletcher and J. Robinson, *Instrumental Methods in Electrochemistry*, Ellis Horwood Limited, Chichester (1985) 206.
22. A. Vorobyova, A.I. Lesnikovich and V.V. Muchinskii, *Colloid. Surface A* **150** (1999) 297.
23. M. Aslam, G. Gopakumar, T.L. Shoba, I.S. Mulla, K. Vijayamohanam, S.K. Kulkarni, J. Urban and V. Vogel, *J. Colloid. Interf. Sci.* **225** (2002) 79.
24. Zhong-shan Hong, Yong Cao and Jing-fa Deng, *Mater. Lett.* **52** (2002) 34.
25. Hui Wang, Jin-Zhong Xu, Jun-Jie Zhu and Hong-Yuan Chen, *J. Cryst. Growth* **244** (2002) 88.
26. M.L. Farquhar, J.M. Charnock, K.E. England and D.J. Vaughan, *J. Colloid. Interf. Sci.* **177** (1996) 561.
27. A.F. Lee, D.E. Gawthrope, N.J. Hart and K. Wilson, *Surf. Sci.* **548** (2004) 200.
28. K. Shibagaki and S. Motojima, *Carbon* **38** (2000) 2087.
29. E. Ferjani, M. Mejdoub, M.S. Roudesli, M.M. Chehimi, D. Picard and M. Delamar, *J. Membrane Sci.* **165** (2000) 125.
30. C.D. Wagner, W.M. Riggs, L.E. Davis, J.F. Moulder and G.E. Muilenberg, *Handbook of X-ray photoelectron spectroscopy*, Published by Perkin-Elmer Corporation, Physical Electronic Division, 6509 Flying Cloud Drive, Eden Prairie, Minnesota 55344, USA, 1979.
31. H. Piao, K. Adib and M.A. Barteau, *Surf. Sci.* **557** (2004) 13.
32. Yu Ying, Li-Li Ma, Wen-Ya Huang, Jia-Lin Li, Po-Keung Wong and Jimmy C. Yu, *J. Solid State Chem.* **178** (2005) 1488.